Transendothelial Transport of Serum Albumin: A Quantitative Immunocytochemical Study

L. Ghitescu and M. Bendayan

Département d'Anatomie, Université de Montréal, Montréal, Québec, Canada H3C 3J7

Abstract. The steady-state distribution of endogenous albumin in mouse diaphragm was determined by quantitative postembedding protein A–gold immunocytochemistry using a specific anti–mouse albumin antibody. Labeling density was recorded over vascular lumen, endothelium, junctions, and subendothelial space. At equilibrium, the volume density of interstitial albumin was 18% of that in circulation. Despite this large difference in albumin concentration between capillary lumen and interstitium, plasmalemmal vesicles labeling was uniformly distributed across the endothelial profile. 68% of the junctions displayed labeling for albumin, which was however low and confined to the luminal and abluminal sides. The scarce labeling of the endothelial cell surface did not confirm the fiber matrix theory. The kinetics of albumin transcytosis was evaluated by injecting radioiodinated and DNP-tagged BSA. At 3, 10, 30, and 60 min, and 3, 5, and 24 h circulation time, blood radioactivity was measured and diaphragms were fixed and embedded. Anti-DNP antibodies were used to map the tracer in aforementioned compartments. A linear relationship between blood radioactivity and vascular labeling density was found, with a detection sensitivity approaching 1 gold particle per DNP-BSA molecule. Tracer presence over endothelial vesicles reached rapidly (10 min) a saturation value; initially localized near the luminal front, it evolved towards a uniform distribution across endothelium during the first hour. An hour was also needed to reach the saturation limit within the subendothelial space. Labeling of the junctions increased slowly, out of phase with the inferred transendothelial albumin fluxes. This suggests that they play little, if any, role in albumin transcytosis, which rather seems to proceed through the vesicular way.

A central point of interest in the biology of the cardiovascular system concerns the transendothelial transport (transcytosis) of plasma molecules. A large amount of data was generated by experiments in which radioactively tagged molecules of different sizes and physiological significance have been injected or perfused in segments of the body or in isolated organs. The vascular permeability was evaluated by measuring the radioactivity collected in lymph, retained in the tissue, or cleared from the circulating fluids (42). The interpretation of these data suggested some models in which the endothelial layer was considered as a passive sieve endowed with pores of different dimensions. Although widely accepted by physiologists, these models, based solely on diffusional and convectional processes, did not completely explain the experimental data regarding the vascular permeability to macromolecules, leaving room for other possible mechanisms of endothelial transport (35). Purely conceptual, these models prompted a considerable number of morphological studies on vascular endothelium in an attempt to directly visualize the transendothelial pathways followed by macromolecules. However, the putative endothelial pore system has not been convincingly identified. At present some investigators support the idea that in endothelium the transcytosis of macromolecules takes place actively, in quanta, via shuttling plasmalemmal vesicles (31, 40). Others suggest that short-lived transendothelial channels formed by either tubular systems (2) or transient fusion of the plasmalemmal vesicles (9) might be the pathway for macromolecular passage. Finally, a third concept advocates for an entirely paracellular passive transport proceeding via interendothelial junctions and modulated by endothelial contractility (10).

With this controversy as a background, recent experimental evidences have suggested that the selectivity of the endothelial transport process might be related to other parameters than simply the charge and the size of the transported molecules. Specific recognition sites expressed on the endothelial cell surface were proposed as key elements in vascular permeability to insulin (24), low density lipoproteins (18, 44) ceruloplasmin (20), and transferrin (21, 41). Even albumin, the most abundant plasma protein, was suggested to be transported across the endothelium by a receptor-mediated mechanism (39). All these models emerged from experiments performed either in situ by perfusing the tracers, or in vitro using cultured endothelial cells. It has been shown however that the presence of plasma proteins (11, 37, 43) or even platelets (38) within the vascular lumen greatly influences the selectivity and the rate of the transen-

dothelial transport. Therefore, studies performed in conditions as close as possible to the natural ones are required in order to confer physiological significance to the findings. Both immunocytochemistry and autoradiography have been used to detect the presence of serum albumin within endothelial plasmalemmal vesicles and subendothelial space (1, 6, 34, 50). These qualitative approaches have shown that interstitial albumin distribution varies from one tissue to another. Apparently some types of vascular endothelial cells restrict the passage of serum albumin, while others exhibit different degrees of permeability even within the same anatomical entity (15, 17).

The development of the protein A–gold immunocytochemical technique (3) opened the possibility to measure with high resolution the presence of various antigens, and quantitative data concerning the steady-state distribution of endogenous albumin within several tissues have already been reported (4, 26). We have decided to perform a quantitative investigation of the dynamics of transendothelial albumin transport in relation with the associated ultrastructural endothelial features, by using postembedding quantitative protein A–gold immunocytochemistry.

Materials and Methods

Crystallized BSA and mouse albumin (Fr.V) were purchased from Sigma Chemical Co. (St. Louis, MO); 2,4,dinitrobenzene sulfonic acid was from Aldrich Chemical Co. (Milwaukee, WI); ^{125}I-Na, carrier free was from ICN Biochemicals (Missisauga, Ontario, Canada); and chloramine T immobilized on polystyrene beads (Iodo-Beads) was from Pierce Chem. Co. (Rockford, IL).

Rationale of the Experiments

The approach consisted of two main steps. The first one addressed the endogenous albumin steady-state distribution measured in mouse diaphragm. Albumin epitopes being quite sensitive to chemical fixation and particularly to osmium, the specimens had to be fixed with aldehydes only and embedded at low temperature in a hydrophylic resin. This stage provided the reference values for a second one in which we monitored the transendothelial passage of an exogenous albumin directly injected in the bloodstream. To discriminate the tracer from the endogenous albumin pool, the injected exogenous albumin was tagged with a hapten (dinitrophenol). This procedure has the advantage to render the tracer easily detectable even under a relatively harsh fixation including OsO_4 (33) which optimally preserved the ultrastructural details.

Preparation of the Tracer

BSA was tagged with dinitrophenol according to the method of Little and Eisen (25). In brief, 1,600 mg albumin dissolved in 80 ml water containing 400 mg K_2CO_3 were reacted for 24 h at 20°C with 800 mg 2,4,dinitrobenzene sulfonic acid. After dialysis against 10 mM phosphate buffer, pH 7.2, containing 0.85% NaCl (PBS), a monomeric dinitrophenylated albumin (DNP-BSA) fraction was obtained by Sephadex G-200 gel chromatography. This fraction was concentrated by ultrafiltration to 120 mg/ml and was characterized by PAGE in nondissociating conditions (12) and by IEF in 1% Agarose IEF (Pharmacia LKB Biotechnology, Uppsala, Sweden). The average number of DNP residues introduced per BSA molecule was spectrophotometrically evaluated using a molar extinction coefficient of 17,530 at 360 nm for DNP-lysyl (25) and a molecular weight of 66,000 for albumin. DNP-BSA was radioiodinated using Iodo-Beads according to manufacturer's instructions to a final specific activity of 233 cpm/μg protein as measured in a liquid scintillation spectrometer (model 8000; Beckman Instrs. Inc., Fullerton, CA). Less than 2% of the activity was soluble in 10% TCA. DNP-BSA concentration was determined by Coomassie brilliant blue (7) and amido black 10B (36) binding methods, against a BSA standard, in order to test for any interference of DNP with the development of the colorimetric reaction by the protein. Both methods gave identical results.

Immunocytochemical Detection of Endogenous Albumin

Six CD-1 male mice, 30–35 *g* body weight, fed ad libitum were killed by cervical dislocation. The diaphragms were fixed in situ for 15 min in 2.5% formaldehyde, 1.5% glutaraldehyde in 100 mM phosphate buffer at 37°C, removed, cut in small blocks, further fixed in fresh aldehydes for 1 h, dehydrated, and embedded in Lowicryl K4M at −20°C (3). Thin sections were quenched in 150 mM glycine, and sequentially incubated in rabbit anti-mouse albumin antiserum (Sigma Chem. Co.) (2 h, 1:1,000 dilution) and protein A conjugated with gold of 10-nm particle diameter (14) (30 min, protein A–gold at A_{520} = 0.5). After staining with uranyl acetate and lead citrate the sections were examined in a Philips 410 electron microscope operating at 80 kV. Controls for the specificity of the immunostaining consisted of sections incubated with either normal rabbit serum, protein A–gold only, or the antialbumin antiserum preabsorbed with 0.1% mouse albumin.

Immunocytochemical Detection of DNP-BSA

After ether anesthesia, 400 μl of blood was withdrawn from the common iliac vein of the mice, by using a No. 30 hypodermic heparinized needle. The blood was immediately replaced by injecting the same volume of prewarmed (37°C) concentrated radioiodinated DNP-BSA (120 mg/ml). The syringes were weighted before and after the procedure. The whole operation took 60–120 s. For each animal a drop of blood was collected at 3 min after injection from the cut tail tip and 20 μl was counted in duplicates by liquid scintillation spectrometry. At 3, 10, 30, and 60 min and at 3, 5, and 24 h the animals were killed by cervical dislocation and the diaphragms were fixed in situ for 15 min, and then overnight at 4°C with aldehydes, postfixed for 90 min in 1% cold OsO_4 in 100 mM phosphate buffer, dehydrated slowly in graded ethanol to minimize tissue shrinkage, and embedded in Epon 812. Just before killing, two 20-μl blood aliquots were collected and counted in order to measure the amount of circulating radiolabeled DNP-tagged tracer. To measure the vascular and total volumes in which our tracer was dispersed, five mice were injected with 100 μl of ^{125}I-DNP-BSA (8.9×10^6 cpm) mixed with ^{51}Cr-labeled mouse erythrocytes (32) (2.14×10^4 cpm) at 50% hematocrit. After 10 min of circulation, blood aliquots were differentially counted for the two isotopes in a gamma counter (model 8000; Beckman Instrs. Inc.), data being corrected for the partial energy overlap. The vascular volume and the apparent volume of distribution for DNP-BSA at 10 min were calculated from the ratios between the measured radioactivity for ^{51}Cr and ^{125}I, respectively, and the corresponding injected specific activities of the two isotopes.

50-nm thin sections of the embedded specimens were quenched for 30 min in PBS containing 1% ovalbumin, and incubated for 2 h in anti-DNP IgG (Dako Corp., Carpinteria, CA) diluted 1:4,000 in ovalbumin-containing PBS, followed by 30 min in protein A–gold (A_{520} = 0.5).

Samples of kidney and liver from some animals were similarly fixed and processed in order to check for possible losses of circulating tracer by abnormal proteinuria or excessive endocytosis in the reticuloendothelial system.

The specificity of labeling for DNP in relation to the endogenous albumin was assayed by incubating in a similar manner sections of diaphragms derived from control animals which were not injected with the tracer.

Morphometric Analysis of the Labeling

Randomly sampled capillary profiles, at least 100 μm away from the mesothelial layer were examined for each experimental condition. Images of the capillary lumen and of the endothelial profiles together with the interstitial space defined by the endothelium and the adjacent muscle were recorded at a magnification of 31,000. The density of labeling over the vascular lumen, endothelium (nuclear zone excluded), subendothelial space, and the interendothelial junctions was measured using a Videoplan 2 Image Analysis System (Carl Zeiss Canada Ltd., Don Mills, Ontario) and expressed as number of gold particles per unit surface (μm^2) of the analyzed compartment. The final magnification given by the whole system was calibrated using a test grid (Ted Pella Inc., Redding, CA).

To evaluate the efficiency of the immunodetection, the number of albumin molecules theoretically exposed at the surface of the sections over the vascular lumen was calculated and compared with the actual recorded density of labeling. If albumin molecules were considered as prolate ellipsoids with axes of 14 × 4 nm (49), the number of profiles cut per unit of section area (N_A) should be related to the number of objects per unit volume (N_v) by the equation $N_v = N_A^{3/2}/\beta V_v^{1/2}$ (47); V_v represents the fractional volume of the objects and β is a shape coefficient depending on the geometrical

parameters of the ellipsoids. For the given albumin axis β equals 2.15 (48). The numerical density N_v of endogenous albumin was calculated from a concentration of 33.8 mg/ml in mouse serum (5), while that of DNP-BSA was inferred from the measured radioactivity of the blood, taking an average hematocrit value of 45.0% (5). V_v was estimated by multiplying N_v by the volume of a prolate ellipsoid of geometrical parameters of albumin (938 nm^3). Finally, the number of albumin molecules presumed to be laid free on the section surface was corrected by a factor of 0.5 to account for the symmetrical partition of the molecules between the two faces of the cleavage plane (22).

Results

Endogenous Albumin

A strong signal was recorded over the lumen of vascular capillaries in Lowicryl-embedded sections incubated with anti-mouse albumin antiserum (Fig. 1 *A*). Gold particles were also detected in plasmalemmal vesicles of the endothelium (Fig. 1 *B*) and in the subendothelial space. No

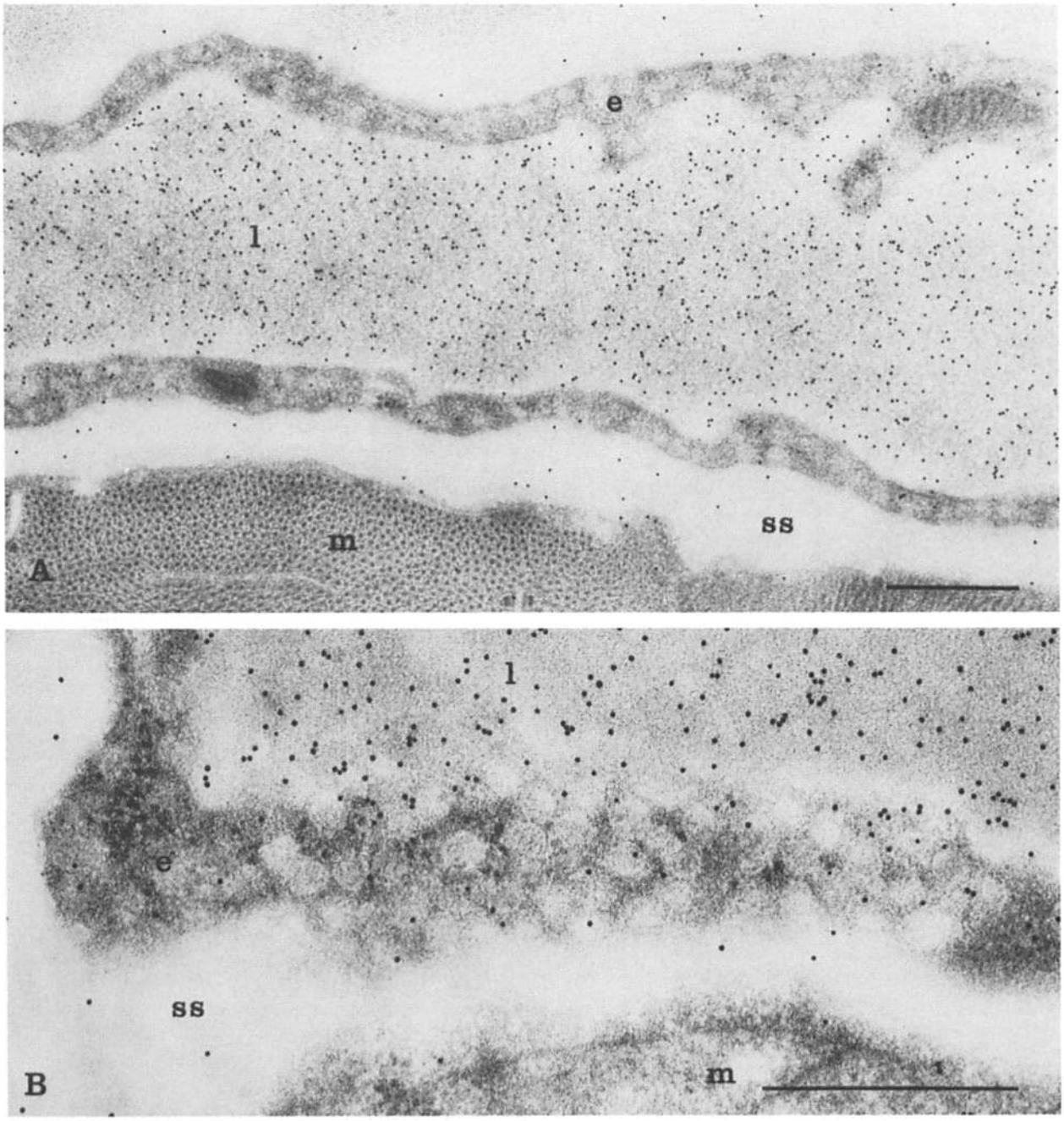

Figure 1. Immunocytochemical detection of endogenous albumin distribution in the capillary bed of mouse diaphragm. The density of labeling in the pericapillary space is approximately five times lower than that encountered in the vascular lumen (*A*). Most of the gold particles are associated with the plasmalemmal vesicle profiles (*B*). *e*, endothelium; *l*, lumen; *m*, muscle; *ss*, subendothelial space. Bar, 0.5 μm.

particular decoration of the luminal plasmalemma proper of the endothelial cells was observed throughout the examined specimens. Very little background was associated with erythrocytes or muscle cells.

Incubation of the specimens with either immune serum preabsorbed with mouse albumin, or normal rabbit serum followed by protein A–gold, or with protein A–gold alone gave no labeling, substantiating the specificity of the endogenous albumin immunodetection.

The morphometric analysis of the labeling in each of the above-mentioned compartments (Table I) revealed a large difference between the luminal and the interstitial concentrations of endogenous albumin. Apparently less than one fifth of the labeling density recorded within the capillary lumen was encountered within the subendothelium. However, in spite of the fact that vascular and abluminal fronts of the endothelial cells were exposed to such dissimilar conditions, the labeling associated with endothelium was rather uniformly distributed across its profile (Fig. 2, *bottom*). This distribution was assessed by measuring the ratio between the distance separating each gold granule from the luminal plasmalemma (D_T) and the endothelial thickness (D_E) at that site (Fig. 2, *top*). 68% of the junctional profiles were labeled but the intensity of the labeling was relatively low (between 1 and 4 gold particles per junction) (Fig. 3). The distribution of the label along the interendothelial clefts was evaluated by the ratio R between the position of the gold particle with respect to the luminal opening L_T and the total length L_J of the junction (Fig. 4 *A*). This analysis has shown that most of the albumin detected within the space between adjacent endothelial cells was preferentially located towards either the luminal or the abluminal openings, while only 18% of the junction-associated signal was detected in the middle portion of the slits with a striking interruption relatively close to the abluminal side (Fig. 4 *B*).

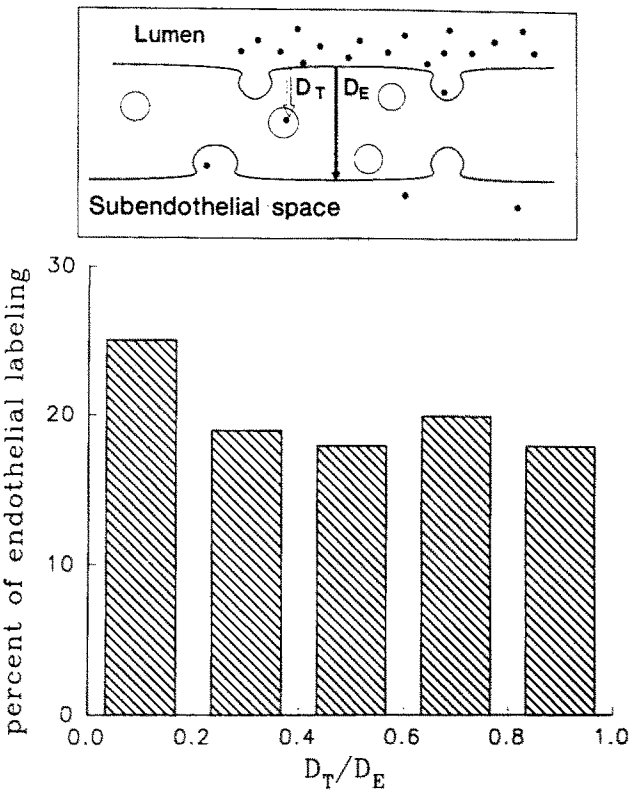

Figure 2. Localization of the endogenous albumin-specific label across the capillary endothelial profile. By taking the endothelial vascular front as a space origin, the relative position of each gold particle was defined by the ratio D_T/D_E (*top*). Histogram depicting the relative spatial distribution of 887 gold particles randomly recorded over the endothelium (*bottom*). The values of 0 and 1 on the abscissa represent particles localized at the luminal and abluminal fronts, respectively.

Exogenous Tracer

Tracer Characterization. Under the relatively mild conditions used for BSA dinitrophenylation, only 10 out of the 57 lysyl groups of albumin were tagged by DNP. This extent of dinitrophenylation is known to induce relatively few changes in albumin conformation (23). However, DNP-BSA become slightly more anionic (pI 4.6) than the native variant (pI 4.9) (Fig. 5 *A*). As a result of gel filtration, the injected tracer was devoid of polymers or aggregates, and was rather uniformly loaded with DNP, as demonstrated by the single band revealed by electrophoresis in nondissociating conditions (Fig. 5 *B*).

Table I. Labeling Density Distribution for Endogenous Albumin

Compartment	Vascular lumen	Endothelial profile	Subendothelial space	Background
Labeling density* (particles/μm^2)	227 ± 6.7	26.7 ± 1.0	41.6 ± 1.4	3.0 ± 0.3
	(n = 37)	(n = 260)	(n = 260)	(n = 40)
Percentage of circulating albumin	100%	11.8%	18.3%	1.3%

Background was measured over the muscle. Morphometry performed on control sections incubated with immune serum preabsorbed with mouse albumin gave 2.3 ± 2.8, 1.1 ± 2.3, and 2.4 ± 2.2 gold particles/μm^2 over capillary lumen, endothelium, and interstitium, respectively (n = 40 for each).
* mean ± SD of the mean.
n, number of profiles examined.

Controls of the Tracer Administration and Detection. The uniformity of the amount of tracer administered to the animals was checked both by the weight of the injected dose (431 ± 9.8 mg/mouse) and by the blood radioactivity retrieved from each animal after 3 min of circulation (2,232 ± 180 cpm/μl, n = 11). The average blood volume in which the tracer was initially dispersed was 2.26 ± 0.15 ml (n = 5), according to the dilution of the ^{51}Cr-labeled erythrocytes coinjected with the DNP-BSA in some animals.

The anti-DNP antibodies did not recognize the endogenous proteins; no signal was elicited on sections derived from animals which have not received DNP-BSA.

Very few gold particles were found associated with the endocytic structures of liver reticuloendothelial cells or were restricted to the lamina rara interna of the renal glomerular basement membrane (not shown). This demonstrates that the tracer was not cleared from circulation by the liver or excreted in significant amounts.

DNP-BSA Localization within the Tissue. A quite uniform density of gold particles was observed within the lumen of the capillary profiles indicating a general recruitment of blood vessels. With increasing circulation time, the signal intensity steadily declined reaching 8% of the original one af-

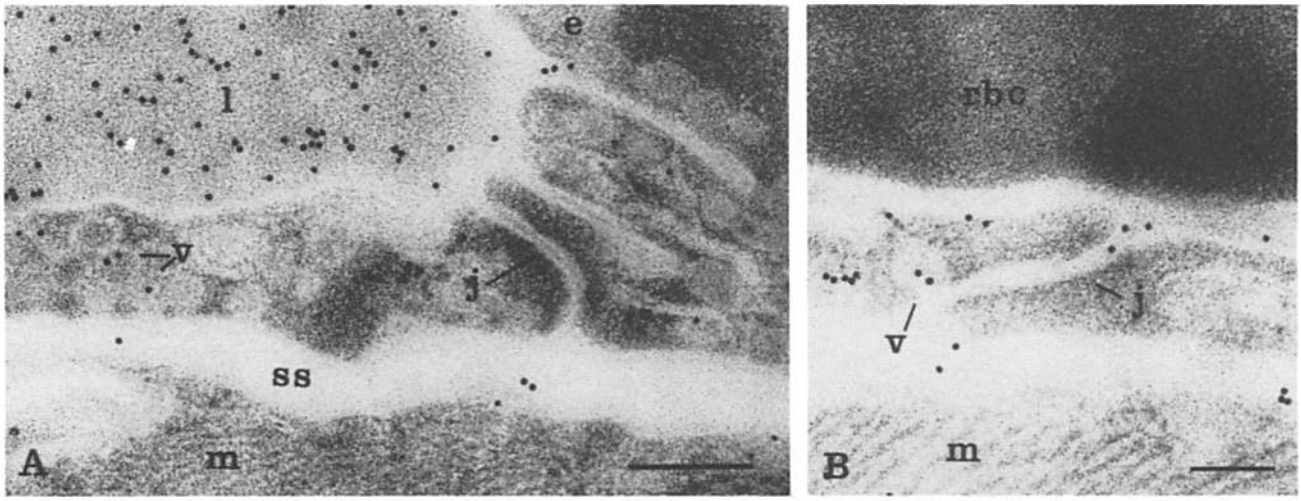

Figure 3. Endogenous albumin presence over the interendothelial junctional profiles. Approximately 32% of the 323 examined junctions were unlabeled (*A*), while the rest of 68% contained up to 4 gold particles per interendothelial space, mostly distributed toward the periphery of the cleft (*B*). *l*, lumen; *j*, junction; *m*, muscle; *ss*, subendothelial space; *v*, vesicle. Bars, 0.2 μm.

ter 24 h (Fig. 6, *A–C*). Over the endothelial cells, the plasmalemmal vesicles were the only labeled structures. No particular association of DNP-BSA with the endothelial plasmalemma proper, endosomes, or lysosomes was observed.

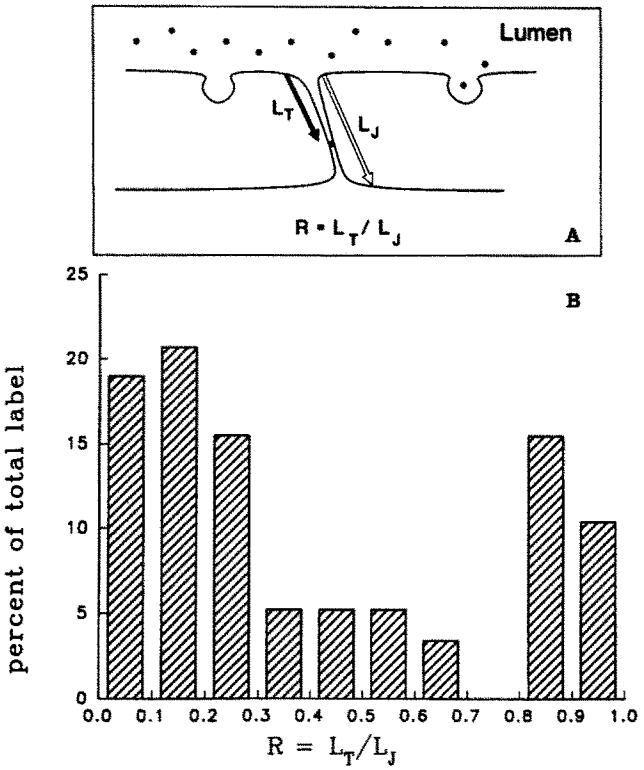

Figure 4. Localization of the endogenous albumin-associated label detected over the junctional profiles. The opening of the junction towards the vessel lumen was taken as origin, and the ratio between the distance separating each gold particle from this point and the length of the interendothelial cleft (*A*) was calculated. The accompanying histogram represents the percentage of gold particles having certain relative locations along the junction out of the total label detected over this compartment (*B*). Most of the tracer apparently is confined to the extremities of the clefts.

The position of the labeled plasmalemmal vesicles evolved with time; while initially located near or open to the luminal endothelial front (Fig. 6 *A*), the vesicles detected as carrying DNP-BSA acquired a rather uniform distribution across the endothelial cells at later time points (Fig. 6, *B* and *C*). Some of them appeared in direct continuity with the abluminal plasmalemma. DNP-BSA was detected within the subendothelial space starting even from 3 min. The penetration of the tracer increased with time although large differences between the blood and interstitial space remained always evident. At no moment did the endothelial basement membrane contain more DNP-BSA than the rest of the interstitium. Also the subendothelial regions around the openings of the interendothelial junctions did not appear to be preferentially labeled. Most of the interendothelial clefts did not appear to contain DNP-BSA, although in their proximity vesicular structures did carry the tracer (Fig. 7). Only 15% of the 425 examined endothelial junctions were labeled at 10 min after tracer injection. The incidence of the labeled junctional profiles increased with circulation time, but none of them displayed a decoration pattern suggestive of a continuous transendothelial pathway for DNP-BSA. A sustained but not a systematical survey of the venular profiles did not reveal the tracer as leaking through open junctions in these vascular segments.

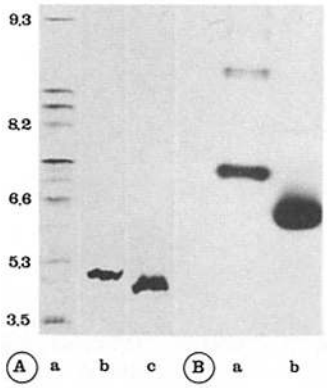

Figure 5. Biochemical characterization of DNP-BSA tracer. (*A*) IEF of native BSA (*b*) and DNP-BSA (*c*) in relation to markers of different pI (*a*). (*B*) Comparative electrophoresis in nondissociating conditions of native (*a*) and dinitrophenylated albumin (*b*), demonstrating that the injected tracer contains no polymers or aggregates.

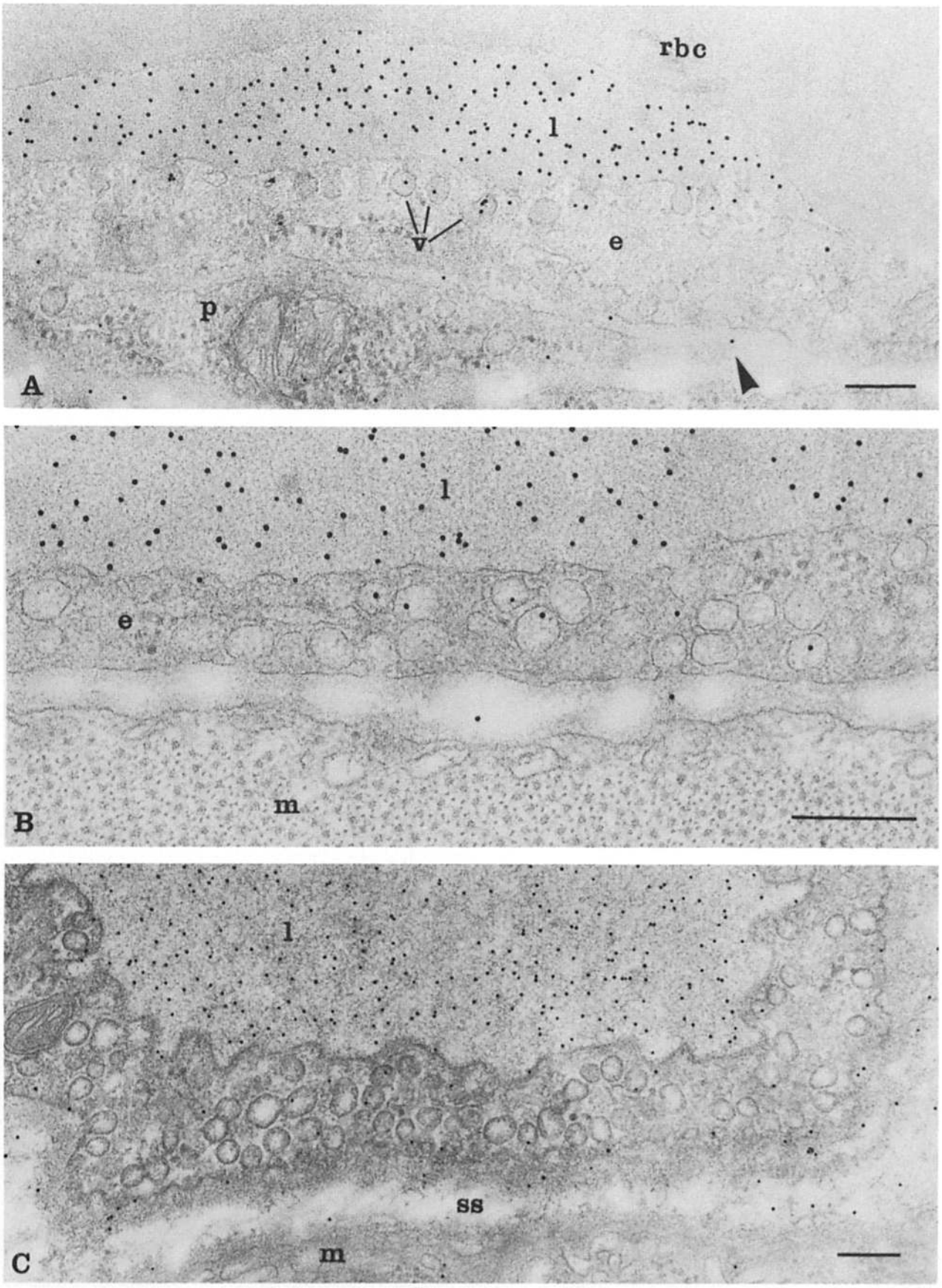

Figure 6. Representative sequence of DNP-BSA immunodetection at 3 (*A*), 10 (*B*), and 60 min (*C*). The labeled plasmalemmal vesicles appear to redistribute in time across the endothelial cells. *e*, endothelium; *l*, lumen; *m*, muscle; *p*, pericyte; *rbc*, red blood cell; *ss*, subendothelial space; *v*, plasmalemmal vesicle. Bars, 0.2 μm.

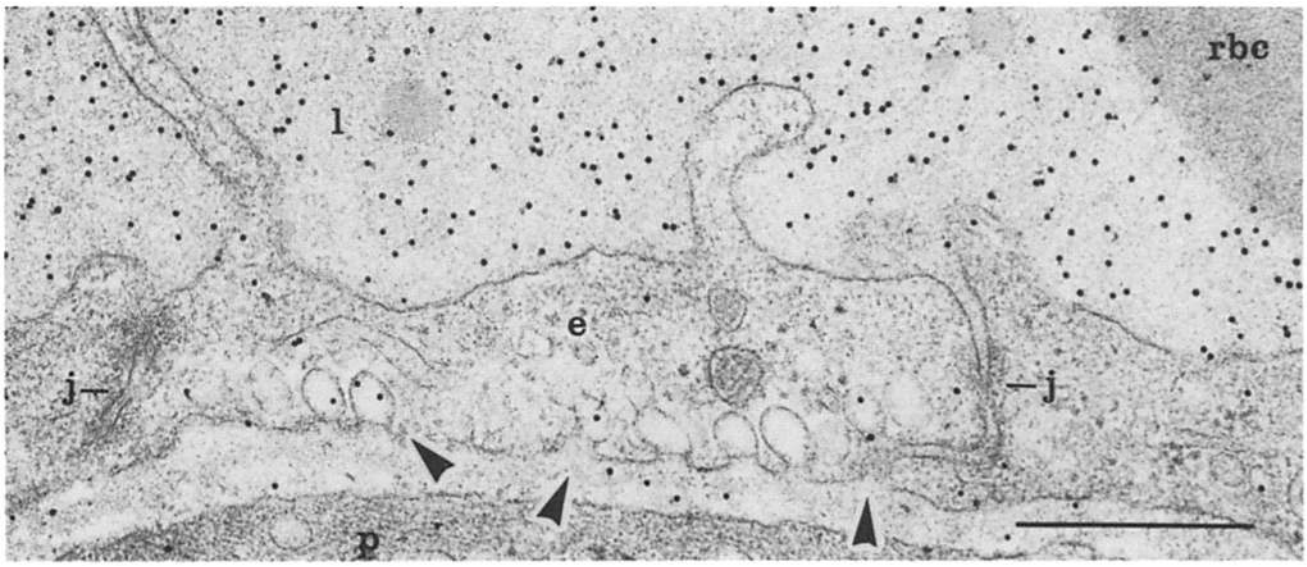

Figure 7. At 10 min after DNP-BSA injection most of the junctions do not contain tracer, while in their proximity labeled vesicles (*arrowheads*) appear to discharge their content into the subendothelial space. *j*, junction; *l*, lumen; *p*, pericyte; *rbc*, red blood cell. Bar, 0.2 μm.

Morphometric Analysis of the Labeling. The reliability of our quantitative immunocytochemical approach was substantiated by the relationship between the intensity of the immunolabeling and the concentration of the detected antigen (DNP-BSA). The specific radioactivity of the blood (Λ – cpm/μl) at the moment of the sacrifice was therefore correlated with the density of gold particles (N_L – particles/μm²) measured over the capillary lumen. Both ^{125}I-DNP-BSA concentration found in circulation (Fig. 8 *A*) and the labeling density over the blood plasma (Fig. 8 *B*) followed the same decay trend. When correlated by the least square method the two parameters exhibited a nearly perfect fitting ($r = 0.97$) with the equation: $N_L = 32.92 + 0.23\ \Lambda$ (Fig. 8 *C*).

The quantitative data regarding the presence of DNP over the capillary lumen, in endothelial cell profile, and within the subendothelial space are summarized in Table II. The density of labeling associated with blood plasma diminished in time, while the amount of the tracer detected over the entire endothelial profile increased rapidly and reached a saturation value of ~44 particles/μm² in 10 min. This was maintained during the first hour of circulation. At later time points the labeling of the endothelium sloped down, probably in relation with the decrease of the circulating tracer concentration.

The position of the DNP-BSA–labeled plasmalemmal vesicles with respect to the two endothelial fronts was evaluated by the same method used for endogenous albumin. The histogram depicting the relative position of the gold granules within the endothelium (Fig. 9) showed that at 3 min, most of the label was situated close to the vascular lumen. Within the first hour of circulation the tracer slowly reached a uniform transendothelial distribution. Interestingly, starting from 10 min and up to 1 h, the labeling density over the endothelium remained at a rather constant value (Table II), while its spatial distribution evolved toward an homogenous one (Fig. 9).

The measurements made for the presence of DNP-BSA within the subendothelial space have shown that the tracer penetrates this compartment at a comparatively lower rate than that with which the endothelial vesicles are filled (Table II). Although almost one third of the maximal value of the subendothelial labeling was detected as soon as 3 min of circulation, it took up to 1 h for this compartment to reach the saturation level of its labeling.

At variance with the situation found for endogenous albumin, at 10 min DNP-BSA circulation time only 15% of the junctional profiles displayed a certain, usually low degree of labeling (1–2 particles/junction). Apparently, DNP-BSA molecules present in the junctions did not penetrate the whole length of the cleft but were restricted to the extremities (Fig. 10).

Discussion

The goal of this study was to assess by the means of the quantitative immunocytochemistry the validity of the current models regarding the mechanisms of transendothelial albumin passage. Dinitrophenol-tagged heterologous albumin was injected in the mouse bloodstream and detected at different circulation intervals in the blood plasma, endothelium, endothelial junctions, and subendothelial space. As a reference, the distribution of endogenous albumin was also immunocytochemically measured in these compartments.

The relationship between the concentration of the tracer and the corresponding immunolabeling density was tested by injecting iodinated, DNP-tagged BSA and by measuring in parallel the radioactivity of the blood and the immunolabeling density over the vascular lumen. The linear correlation, over a large range, between these two parameters (Fig. 8 *C*) provides direct evidence that the immunocytochemical signal accurately represents the tracer concentration.

Another methodological aspect concerned the immunodetection efficiency for the native or dinitrophenylated albumin forms. In this respect the number of albumin molecules theoretically presumed to be laid free at the surface of the sections, and therefore accessible to the immune reagents, were

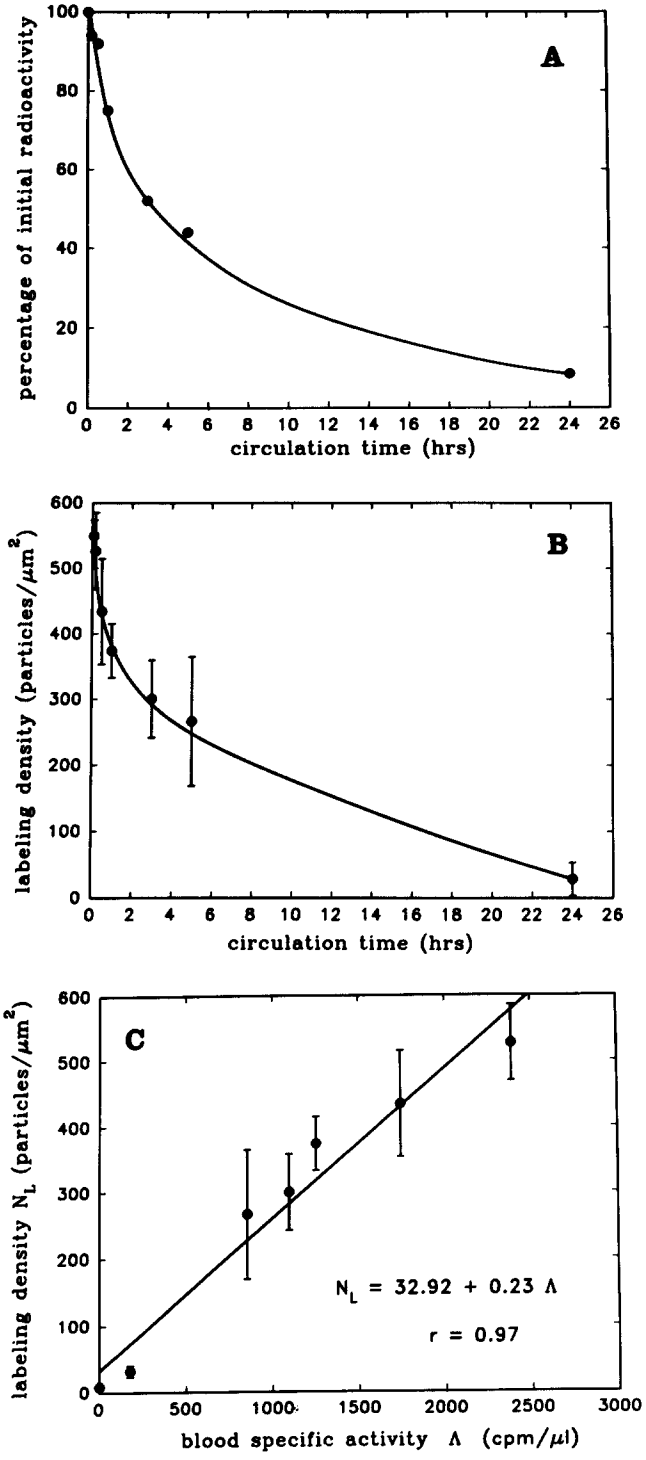

Figure 8. (*A*) Specific blood radioactivity at different times after injection of ^{125}I-DNP-BSA. (*B*) Immunolabeling density recorded over the vascular lumen in the specimens harvested from animals used in *A*. (*C*) Linear relationship between the immunolabeling density and the concentration of circulating DNP-BSA. Bars, standard error.

compared with the corresponding gold particles labeling them. The use of the stereological algorithm outlined in Materials and Methods suggested that ~2,510 endogenous albumin and 645 DNP-BSA molecules (at 10 min after injection) were expected to be exposed per surface unit (μm^2) of the sections passing through the vascular lumen. The corresponding labeling densities obtained by immunocytochemistry were of 227 ± 6.7 and 526 ± 10.8 gold particles/μm^2, respectively (Tables I and II), giving an approximative detection efficiency of 9% for endogenous albumin and 82% for DNP-BSA.

Table II. Compartmental Distribution of the Labeling Density (Gold Particles/μm^2 of Analyzed Profile) for DNP-BSA at Different Circulation Times

Circulation time	Vascular lumen	Endothelial profile	Subendothelial space
Control (not injected)	8.8 ± 0.9*	8.1 ± 0.8	7.8 ± 0.6
3 min	550 ± 10.7	31.4 ± 1.2	21.9 ± 1.6
10 min	526 ± 10.8	43.7 ± 1.5	29.9 ± 1.0
30 min	434 ± 14.2	44.2 ± 1.4	36.5 ± 1.0
1 h	374 ± 7.8	46.9 ± 0.7	64.4 ± 1.58
3 h	300 ± 10.7	25.7 ± 1.1	53.3 ± 1.33
5 h	267 ± 17.1	26.7 ± 1.27	56.6 ± 1.8

Morphometric data without background subtraction are listed. For each time point the measurement was performed on 350–600 capillary profiles.
* Mean ± SEM.

The labeling performed for endogenous albumin revealed its presence within the pericapillary space suggesting, in agreement with previous reports (50), that the microvasculature of the diaphragm is permeable to this protein. However, a strong asymmetry in albumin distribution across the endothelium exists in steady-state conditions; the ratio between corresponding vascular and interstitial labeling densities was of 5.5:1. It had been shown by morphometric studies performed on capillaries of different tissues that the number of vesicles connected to the endothelial surface was equally distributed between the two fronts (16, 27, 29, 30). If these vesicles were to be considered as immobile structures permanently exposed either to the blood, or to the interstitium, the distribution of the label over the endothelial cell profile should follow the asymmetry of albumin concentration in the two extracellular compartments. Instead, the labeled plasmalemmal vesicles were found to be rather uniformly scattered across the endothelium (Fig. 2 *B*), supporting the idea of a vesicular movement.

At variance with other works (6, 37) reporting the detection of a layer of endogenous albumin adsorbed on the endothelium surface, we have observed very few gold particles associated with endothelial plasmalemma proper on both sides of the cell. The difference might be explained by their use of immunoperoxidase as the detection agent, with all the pitfalls of the reaction product delocalization and the lack of quantitative correlation with the density of antigen. Our observation suggests that albumin is not a main component of the putative fibrillar matrix covering the endothelial surface and modulating the vascular permeability (11). Actually, recent physiological measurements have shown that serum factors other than albumin might be responsible for maintaining the microvessel barrier properties at normal values (19).

In vivo injection of DNP-tagged BSA provides a reasonable model for the study of transendothelial transport of albumin. The clearance curve of the tracer from the circulation was similar to that recorded for nondinitrophenylated ^{125}I-BSA (not shown). Moreover, a very low uptake by the

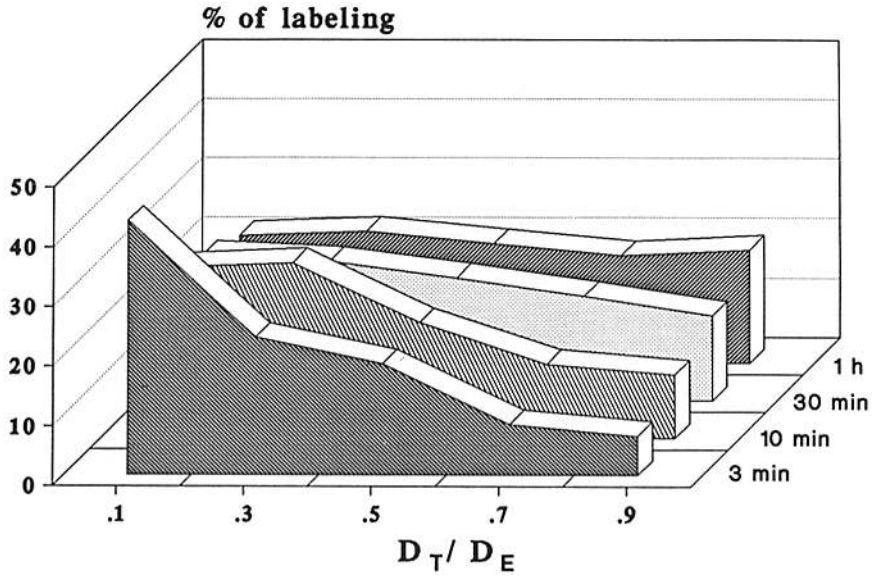

Figure 9. The redistribution of the label recorded over the endothelial cell profile at different intervals after DNP-BSA injection. The labeling density over the endothelium remains constant from 10 to 60 min. The relative position of each endothelial-associated gold granule was assessed as in Fig. 2 (*top*). Between 800 and 1,000 gold particles were counted for each condition.

liver sinusoidal cells, and lack of penetration through the lamina densa of the kidney glomerular basement membrane validated DNP-BSA as a tracer close to the native BSA. The similarity between the endogenous and exogenous dinitrophenylated albumins became even more evident when the labeling densities obtained over the endothelial cells and within the subendothelial space at different moments after injection were expressed as percentage of the corresponding circulating DNP-BSA (Table III). Within both compartments, the relative labeling densities reached at saturation were identical to those found for the endogenous protein.

The transport of DNP-BSA towards the subendothelial space seemed to be a relatively rapid process. Although the total equilibration between the blood and the interstitium took ~1 h, almost one third of the saturation value for DNP-BSA within the subendothelium was reached after 10 min of circulation (Table II). In fact, the apparent volume distributions for ^{51}Cr-labeled erythrocytes and for ^{125}I-DNP-BSA measured at 10 min after injection were of 0.0567 ± 0.0028 ml/g body weight and 0.107 ± 0.0086 ml/g body weight, respectively, which meant that at that time the dilution factor for DNP-BSA was twice as high as for red blood cells. It appears therefore that at the level of the whole organism the albumin egress is remarkably fast. Qualitative morphologic studies have already shown this (28), although they were performed in situ, by perfusing exogenous albumin in the absence of blood elements. Using in vivo experimental models, it has been reported that the pace of albumin turnover between blood and tissue is faster in mice than in other animals, and an equilibration time of 1 h was reported (13).

We did not detect any concentration gradient for DNP-BSA within the interstitial space. Under the assumption that the thin diaphragm tissue is fixed at a reasonable speed, it appeared that the interstitial matrix did not significantly restrict the diffusion of albumin molecules. Also the endothelial basement membrane did not seem to act as a restrictive barrier to the passage of albumin, no particular concentration of either DNP-BSA or endogenous variant being observed in this compartment.

Previous reports have shown that endothelial plasmalemmal vesicles of frog mesenteric capillaries were very rapidly labeled (a matter of seconds) by perfused ferritin (9). Our results demonstrated that in physiological conditions the density of gold particles found to be associated with plasmalemmal vesicles reached rapidly (10 min) a saturation

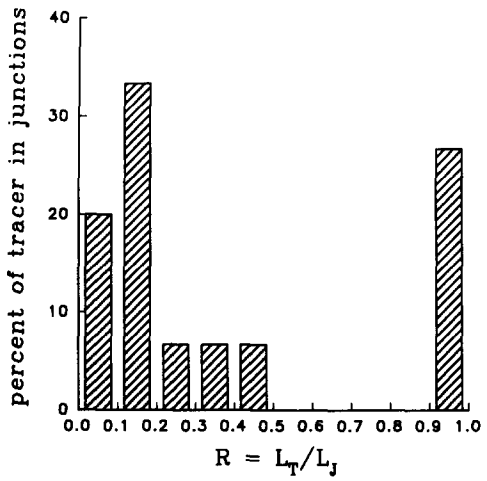

Figure 10. Relative distribution of DNP-BSA in the interendothelial junctional profiles at 10 min after injection. Histogram built according to the procedure outlined in Fig. 4 *A*.

Table III. Endothelial and Interstitial Labeling Densities Expressed as Percentage of Those Found within the Circulation (over the Capillary Lumen) at the Corresponding Circulation Time

	Endothelial profile	Subendothelial space
Endogenous albumin	11.8	18.3
DNP-BSA 3 min	5.7	4.0
10 min	8.3	5.7
30 min	10.2	8.4
60 min	12.5	17.2
3 h	8.5	17.7
5 h	10.0	21.2

value of ~44 particles/μm^2, while the tracer was still close to the vascular front. During the first hour required for the equilibration with the interstitial space, the number of tracer molecules found over endothelial cells did not increase. Instead, the labeled vesicles seemed to slowly acquire a homogenous distribution across the cells (Fig. 9). If a paracellular way was to be the one responsible for albumin extravasation, it would have been expected that the vesicles related to the vascular lumen will be rapidly filled and then, as the DNP-BSA concentration within the subendothelial space increases, the caveolae exposed to abluminal compartment will start to accept the tracer too. Consequently, the number of gold particles over the endothelium should increase in phase with the vascular/interstitial equilibration. Our results contradict this possibility and support the model of a continuous transendothelial movement of a fixed number of tracer-accessible vesicles.

Although from the study on endogenous albumin we did not detect a stream of molecules passing through the endothelial junctions, we could not rule out the interendothelial clefts as a possible transendothelial pathway for albumin, because of the relatively low immunodetection efficiency for this molecule. The possibility that the interendothelial space might be a main contributor to the transcytosis was investigated at short term (10 min) after DNP-BSA injection, when the transendothelial concentration gradient of the tracer as well as the transendothelial DNP-BSA fluxes had both high values. The good immunodetection efficiency for DNP increased the chances of detecting the tracer during its passage through the narrow junctions. Morphometry performed over this compartment has shown however that very few junctions were labeled and the few detected DNP-BSA molecules were located towards the extremities (Fig. 10). The fact that junctional spaces were found to contain a certain amount of endogenous albumin might be interpreted as a result of a slow diffusional process taking place from both endothelial fronts. Our results are in agreement with other data reporting the impermeability of the interendothelial junctions to tracers of different sizes (8, 45, 46), including perfused exogenous monomeric albumin (28). Therefore it appears that in vivo, and at least in the diaphragm, serum albumin does not mainly follow a paracellular route to cross the endothelium. Instead, as suggested by the dynamics of the plasmalemmal vesicle's loading and distribution, the vesicular mechanism for the transcytosis of this protein seems to play the dominant role.

The excellent technical assistance of Diane Gingras, Jean Godbout, and Jean Leveille is gratefully acknowledged.

This research was supported by the Medical Research Council of Canada and by the Heart and Stroke Foundation of Quebec. L. Ghitescu is a recipient of a Medical Research Council Studentship Award.

Received for publication 5 November 1991 and in revised form 30 January 1992.

References

1. Bendayan, M. 1980. Use of Protein A-gold technique for the morphological study of vascular permeability. *J. Histochem. Cytochem.* 28:1251–1254.
2. Bendayan, M., E. Sandborn, and E. Rasio. 1975. Studies of the capillary basal lamina. I. Ultrastructure of the red body of the eel swimbladder. *Lab. Invest.* 37:757–767.
3. Bendayan, M. 1984. Protein A-gold electron microscopic immunocytochemistry: methods, applications and limitations. *J. Electron. Microsc. Tech.* 1:243–270.
4. Bendayan, M., D. Gingras, and P. Charest. 1986. Distribution of endogenous albumin in the glomerular wall of streptozotocin-induced diabetic rats as revealed by high resolution immunocytochemistry. *Diabetologia.* 29:868–875.
5. Bernstein, S. E. 1966. Physiological characteristics. *In* Biology of the Laboratory Mouse. 2nd ed. E. L. Green, editor. McGraw-Hill Inc., New York. 339–350.
6. Bignon, J., P. Chahinian, G. Feldmann, and C. Sapin. 1975. Ultrastructural immunoperoxidase demonstration of autologous albumin in the alveolar capillary membrane and in the alveolar lining material in normal rats. *J. Cell Biol.* 64:503–509.
7. Bradford, M. 1976. A rapid and sensitive method for the quantitation of microgram quantities of protein utilizing the principle of protein-dye binding. *Anal. Biochem.* 72:248–254.
8. Casley-Smith, J. R. 1965. Endothelial permeability II. The passage of particles through the lymphatic endothelium of normal and injured ears. *Brit. J. Exp. Pathol.* 46:35–49.
9. Clough, G., and C. C. Michel. 1981. The role of vesicles in the transport of ferritin through frog endothelium. *J. Physiol. (Lond.).* 315:127–142.
10. Crone, C. 1986. Modulation of solute permeability in microvascular endothelium. *Fed. Proc.* 45:77–83.
11. Curry, F. E., and C. C. Michel. 1980. A fiber matrix model of capillary permeability. *Microvasc. Res.* 20:96–99.
12. Davis, B. J. 1964. Disc electrophoresis. II. Method and application to human serum proteins. *Ann. NY Acad. Sci.* 121:404.
13. Friedman, J. J. 1957. Vascular extravascular equilibration of radioactive iodinated albumin in mice. *Am. J. Physiol.* 101:115–118.
14. Ghitescu, L., and M. Bendayan. 1990. Immunolabeling efficiency of protein A-gold complexes. *J. Histochem. Cytochem.* 38:1523–1530.
15. Ghitescu, L.,Z. Galis, M. Simionescu, and N. Simionescu. 1988. Differentiated uptake and transcytosis of albumin in successive vascular segments. *J. Submicrosc. Cytol. Pathol.* 20:657–669.
16. Gil, J., D. A. Silage, and J. M. McNiff. 1981. Distribution of vesicles in cells of air-blood barrier in the rabbit. *J. Appl. Physiol. Respir. Environ. Exercise Physiol.* 50:334–340.
17. Hart, T. K., and R. M. Pino. 1985. Variations in capillary permeability from apex to cript in the villus of the ileo-jejunum. *Cell Tissue Res.* 241: 305–315.
18. Hashida, R., A. Anamizu, J. Kimura, S. Ohkuma, Y. Youhida, and T. Takano. 1986. Transcellular transport of lipoprotein through arterial endothelial cells in monolayer culture. *Cell Struct. Funct.* 11:31–42.
19. Huxley, V. H., and F. E. Curry. 1990. Differential actions of albumin and plasma on capillary solute permeability. *Am. J. Physiol.* 260:H1645–H1654.
20. Irie, S., and M. Tavassoli. 1986. Liver endothelium desialates ceruloplasmin. *Biochem. Biophys. Res. Commun.* 140:94–100.
21. Jefferies, W. A., M. R. Brandon, S. V. Hunt, A. F. Williams, K. C. Gater, and D. Y. Mason. 1984. Transferrin receptor on endothelium of brain capillaries. *Nature (Lond.).* 312:162–163.
22. Kellenberger, E., M. Durrenberger, W. Villiger, E. Carlemalm, and M. Wurtz. 1987. The efficiency of immunolabeling on Lowicryl sections compared to theoretical predictions. *J. Histochem. Cytochem.* 35:959–969.
23. Kessler, K. F., R. F. Barth, and K. P. Wong. 1982. Physicochemical studies of dinitrophenylated bovine serum albumin. *Int. J. Pept. Protein Res.* 20:73–80.
24. King, G. L., and S. M. Johnson. 1985. Receptor-mediated uptake and transport of insulin by endothelial cells. *Science (Wash. DC).* 227: 1583–1586.
25. Little, J. R., and H. N. Eisen. 1967. Preparation of immunogenic 2,4-dinitrophenyl and 2,4,6-trinitrophenyl proteins. *In* Methodology, Immunology and Immunochemistry. Vol. 1. C. A. Williams and M. W. Chase, editors. Academic Press Inc., New York. 128–133.
26. Londono, I., and M. Bendayan. 1989. Distribution of endogenous albumin across the aortic wall as revealed by quantitative high resolution immunocytochemistry. *Am. J. Anat.* 186:407–416.
27. Mazzone, R. W., and S. M. Kornblau. 1981. Pinocytotic vesicles in the endothelium of rapidly frozen rabbit lung. *Microvasc. Res.* 21:193–211.
28. Milici, A. J., N. E. Watrous, H. Stukenbrok, and G. E. Palade. 1987. Transcytosis of albumin in capillary endothelium. *J. Cell Biol.* 105: 2603–2612.
29. Noguchi, Y., T. Yamamoto, and Y. Shibata. 1986. Distribution of endothelial vesicles in the microvasculature of skeletal muscle and brain cortex of the rat as demonstrated by tannic acid tracer analysis. *Cell Tissue Res.* 246:487–494.
30. Noguchi, Y., Y. Shibata, and T. Yamamoto. 1987. Endothelial vesicular system in rapid frozen muscle capillaries revealed by serial sectioning and deep etching. *Anat. Rec.* 217:355–360.
31. Palade, G. E. 1960. Transport in quanta across the endothelium of blood capillaries. *Anat. Rec.* 136:254.
32. Parker, J. C., H. J. Falgout, R. E. Parker, D. N. Granger, and A. E. Taylor. 1979. The effect of fluid volume loading on exclusion of interstitial albumin and lymph flow in the dog lung. *Circ. Res.* 45:440–450.
33. Pathak, R. K., and R. G. Anderson. 1989. Use of dinitrophenol-IgG conjugates to detect sparse antigens by immunogold labeling. *J. Histochem.*

Cytochem. 37:69–74.
34. Pino, R. M. 1985. Restriction to endogenous plasma proteins by fenestrated capillary endothelium: an ultrastructural immunocytochemical study of the choriocapillary endothelium: *Am. J. Anat.* 172:279–289.
35. Renkin, E. M. 1985. Capillary transport of macromolecules: pores and other endothelial pathways. *J. Appl. Physiol.* 58:315–325.
36. Schaffner, W., and C. Weissmann. 1973. A rapid, sensitive, and specific method for the determination of protein in dilute solutions. *Anal. Biochem.* 56:502–514.
37. Schneeberger, E. E. 1983. Proteins and vesicular transport in capillary endothelium. *Fed. Proc.* 42:2419–2424.
38. Shepard, J. M., D. G. Moon, P. F. Sherman, L. K. Weston, P. J. DelVecchio, F. L. Minnear, A. B. Malik, and J. E. Kaplan. 1989. Platelets decrease albumin permeability of pulmonary artery endothelial cell monolayer. *Microvasc. Res.* 37:256–266.
39. Simionescu, M., and N. Simionescu. 1986. Receptor-mediated transcytosis of plasma molecules by vascular endothelium. *In* Fourth International Symposium on the Biology of Vascular Endothelial Cell. Noordwijkerhout, Abstract Volume, 21 pp.
40. Simionescu, N. 1983. Cellular aspects of transcapillary exchange. *Physiol. Rev.* 63:1536–1579.
41. Soda, R., and M. Tavassoli. 1984. Transendothelial transport (transcytosis) of iron-transferrin complex in the blood marrow. *J. Ultrastruct. Res.* 88: 18–29.
42. Taylor, A. E., and D. N. Granger. 1984. Exchange of macromolecules across the microcirculation. *In* Handbook of Physiology. Vol. IV, Section 2, The Cardiovascular System. E. M. Renkin and C. C. Michel, editors. American Physiological Society, Bethesda, MD. 467–520.
43. Turner, M. R., C. C. Clough, and C. C. Michel. 1983. The effects of cationized ferritin upon the filtration coefficient of single frog capillaries: evidence that proteins in the endothelial cell coat influence permeability. *Microvasc.Res.* 25:205–222.
44. Vasile, E., and N. Simionescu. 1985. Glomerular dysfunction and biopathology of vascular wall. A. L. Copley, Y. Hamashima, S. Seno, and M. A. Ventakachalam, editors. Academic Press, Tokyo. 87–101.
45. Wagner, R. G., and S. C. Chen. 1990. Ultrastructural distribution of Terbium across capillary endothelium: detection by electron spectroscopic imaging and electron energy loss spectroscopy. *J. Histochem. Cytochem.* 38:275–282.
46. Ward, B. J., K. F. Bauman, and J. A. Firth. 1988. Interendothelial junctions of cardiac capillaries in rats: their structure and permeability properties. *Cell Tissue Res.* 252:57–66.
47. Weibel, E. R. 1963. Stereological principles for morphometry in electron microscopic cytology. *Int. Rev. Cytol.* 26:235–302.
48. Weibel, E. R., and D. M. Gomez. 1962. A principle for counting tissue structure on random sections. *J. Appl. Physiol.* 17:343–348.
49. Wright, A. K., and M. R. Thompson. 1975. Hydrodynamic structure of bovine serum albumin determined by transient electric birefringence. *Biophys. J.* 15:137–141.
50. Yokota, S. 1983. Immunocytochemical evidence for transendothelial transport of albumin and fibrinogen in rat heart and diaphragm. *Biomed. Res.* 4:577–586.